Applied Electronics 2008

The First Active Tunable Wideband Impedance Matching Circuit

Balwant Godara[1] and Alain Fabre[2]

[1]Institut Supérieur d'Electronique de Paris (ISEP), 28 rue Notre Dame des Champs, Paris 75006, France
godara@isep.fr
[2]Laboratoire IMS - ENSEIRB, UMR 5218 CNRS, 1 Avenue du Dr. Schweitzer, BP 99, Talence 33402, France
fabre@enseirb.fr

Abstract – **The first transistor-based impedance matching circuit for radio-frequency (RF) applications is introduced in this paper. It adapts arbitrary output impedances of RF blocks to desired values between 50Ω and 250Ω, from 0 to 5GHz, while occupying only 0.005mm² of circuit area in a 0.35µm SiGe BiCMOS process. Its superiority over traditional passive-element networks can be resumed by the following facts: flexible performance without the need for redesigning the components; adaptation of arbitrary impedances to desired values by the simple means of biasing current; extremely small form factors (the smallest observed); and matching over several gigahertz. Application to a low-noise amplifier validates the new topology.**

Index Terms **— Active impedance matching, current conveyors, SiGe BiCMOS, wideband matching.**

INTRODUCTION

The importance of impedance adaptation in wireless receivers cannot be overstated. Individual transceiver components are often fabricated in different technologies, giving rise to multi-chip architectures. For these components (or sub-systems) to be compatible, they must present terminating impedances that are compatible.

This article is dedicated to impedance matching circuits. Section II will be a brief reminder of the basic principle of impedance. Section III will serve as a review of impedance adaptation circuits encountered in wireless systems. It will be observed that matching relies entirely on passive components like inductors, transformers and quarter-wavelength lines. Section III will also serve as a backdrop against which a novel transistor-based ("active") output impedance matching circuit will be proposed and presented (section IV). This new method makes use of the second generation controlled current conveyor (CCCII) as its building block. In-depth analyses of the new method and its simulated performance will be presented in section V. An application example for the new matching circuit will be presented in section VI. It will be shown that the new circuit effectively matches the output of the amplifier, without deteriorating its other parameters. Measurement results on the fabricated circuit will be presented in section VII. The conclusions will highlight the novelty of the new approach by comparing it with traditional matching circuits.

BASICS OF IMPEDANCE MATCHING

A. Scattering Parameters

For a two-port circuit, with an input (port 1) and an output (port 2), represented in fig. 1, the impedances at the input and the output, Z_{IN} and Z_{OUT}, respectively determine the degree of matching to the source and load. The degree of (mis)match between these impedances is represented in terms of the scattering parameters of the two-port. The relevant reflection parameters are S_{11} at the input and S_{22} at the output, defined as:

$$S_{11} = \frac{Z_{IN} - Z_S}{Z_{IN} + Z_S} \quad (1)$$

$$S_{22} = \frac{Z_{OUT} - Z_L}{Z_{OUT} + Z_L} \quad (2)$$

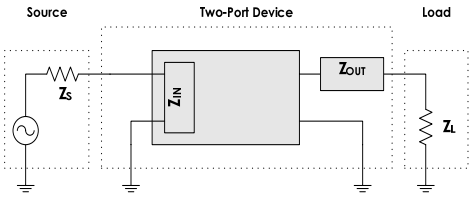

Figure 1 : Impedance matching in a two-port device : Z_{IN} needs to be matched to Z_S and Z_{OUT} to Z_L

S_{11} and S_{22} are generally characterised in decibels ($S_{11,dB} = 10*\log_{10}(S_{11})$). Impedance match is considered successful if the corresponding scattering parameter (S_{11} or S_{22}) is lower than -10dB in the desired frequency range [1].

B. Importance of Impedance Matching

All wireless transceivers contain a multitude of components connected end-to-end. Losses can occur in the signal as it advances from one component to another if the output impedance of the first is not matched to the input of the second. In order to normalise interfacing between transceiver components, a 50Ω standard is normally adopted. Impedance matching assumes heightened importance in the analog section of the transceiver.

Among the main requirements on the performance of RF low-noise amplifiers (LNAs) are low noise, high linearity, sufficient gain, and stable (and purely resistive) Z_{IN} [2]. Matching is necessary to avoid signal reflections on cables,

and minimise alterations of the characteristics of the passive off-chip RF filter which precedes the LNA [3]. Increasingly, LNAs are also required to be wide-band, in order to support various standards from the same device. This places an extra demand on the matching of the LNA ports: it too is required to be wideband [1],[4],[5].

In most transceiver blocks, but especially in the RF section, noise performance is a critical parameter. The best noise performance is usually attained at an optimum Z_S which is often not equal to the complex conjugate of Z_{IN}. However, $Z_S = Z_{IN}^*$ is necessary for a good impedance match and consequently a good power transfer. This suggests a trade-off between noise performance and power transfer [3],[6]. The matching network at the input greatly determines the noise figure [7]. Output port mismatches limit the bandwidth and linearity.

OUTPUT IMPEDANCE MATCHING CIRCUITS

Four methods, all of which exclusively use passive elements, dominate the field of impedance matching solutions: inductor-capacitor (LC-) networks, resistive feedback loops, transformers and quarter-wavelength (λ/4) based networks.

Different topologies are generally adopted for input and output matching circuits, since the demands made on each are specific [5],[7]. Since this article hopes to advance the state of the art in output matching circuits, only these will be considered here.

A. Review of existing matching circuits

LC-based circuits are the most popular among the four categories. Matching is generally obtained using a tank circuit [8]. A shunt-inductor/series-capacitor combination simultaneously sets R_{OUT} and tunes out X_{OUT} [9],[10]. At microwave frequencies, wideband LC matching circuits are easier to realise [11]. Inductor sizes in LC networks are sometimes too high for them to be included on-chip. Even when this is possible, on-chip inductors consume large circuit areas. The physical size of the inductors becomes comparable to that of the transistor, making it difficult to establish a low parasitic connection between the two [12]. This is aggravated when more than one inductor makes up the matching circuit: extra inactive area is required to accommodate adequate separation between the inductors [1],[13].

As with the input, matching of Z_{OUT} can also be achieved using multiple feedback loops composed of resistances. A representative case, presented in [14], achieves good matching from 0.5 to 10GHz.

An ideal 1:n transformer can be used to convert the output impedance of a circuit to a desired value. Unfortunately, on-chip spiral transformers are very lossy and degrade performance [12]. They also suffer from imprecise modelling, leading to large discrepancies between modelled results and real performance [15].

The simplest method of obtaining impedance transformation consists in using the quarter-wavelength transformer. Perfect matching is only achieved at the centre frequency, where the circuit exhibits a reflection zero. High-bandwidth variants of this principle are comprised of multiple λ/4 sections, with multiple reflection zeros. These transformers are limited to applications where the impedance transformation ratio is small [16]. The superiority of line-based output impedance transformers becomes evident at frequencies exceeding 10GHz [17]. Even when they are viable for RF applications, line-based solutions are typically too bulky to be included on-chip.

B. Need for New Solutions

Besides exhibiting drawbacks unique to each, all the topologies presented above suffer from a common problem : once the passive elements' values are chosen, and once they are integrated (or kept off-chip), it is not possible to change their performance. A change in the matching requirement necessitates a re-designing of the matching. This also means that a matching circuit can only be used for the specific application for which it has been designed.

New solutions thus have to be sought which are compatible with the five-pronged demand of low operating voltages, wide bandwidth, small form factors, high potential of integration and ease of performance control. None of the existent solution satisfies these criteria.

At present, transistor-based matching circuits do not exist. If such a topology were envisaged, it would present: high capacity for on-chip integration, small form factors, and versatility. Moreover, a transistor-based structure would be free from the narrow bandwidths inherent to passive matching networks. Even though transistors are used to match impedances in existent literature, the output matching almost invariably uses at least one passive element besides the transistor, most often a LC combination [1]-[3],[5]-[8],[10],[11],[13],[18]. The disadvantages of these partially-passive solutions are the same as the ones mentioned above for each class of solutions. Moreover, the matching in these references is an integral part of the active circuit itself. It is impossible to control this transconductor-based circuit without modifying the core performance.

The section below presents the first all-active wideband impedance-matching circuit. This new solution is based on the properties of the current conveyor, which are here used as transconductor. We have not yet come across a radiofrequency element in which this topology has been effectively used.

NEW TRANSISTOR-BASED MATCHING CIRCUIT

The new approach consists in using second generation controlled current conveyors (CCCII).

A. Circuit Design

Fig. 2 shows the conveyor in voltage follower mode. The signal to be adapted, V_{IN}, is fed at port Y ($V_{IN} = V_Y$), whose characteristic impedance Z_Y consists of a large resistance R_Y in parallel with a capacitance C_Y.

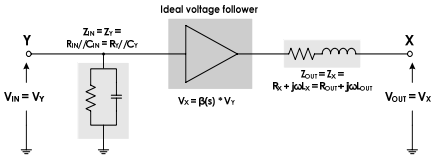

Figure 2 : Block-level representation of the CCCII as impedance matching circuit

R_Y is thus considered an open circuit. (The verity and significance of this supposition will be confirmed later.) The output is tapped at port X ($V_{OUT} = V_X$). The transfer function that characterises the ideal voltage follower (with X port left open) is:

$$\beta(s) = \frac{V_X}{V_Y}(s) = \frac{V_{OUT}}{V_{IN}}(s) \qquad (3)$$

The output impedance, that of port X, consists of a resistance R_X in series with an inductance L_X. In controlled current conveyors, R_X can be controlled by changing the biasing current I_O of the circuit [19]-[22]. The voltage follower thus acts as an impedance conversion circuit: it allows an arbitrary impedance (before port Y) to be adapted to a desired value.

C. Description of the Circuit

Fig. 3 presents the transistor-level diagram of the impedance matching circuit. The core of the impedance conversion circuit is composed of two types of transistors: bipolar NPN transistors Q_1 and Q_3, and PNP transistors Q_2 and Q_4. The elements in the trans-linear loop treat the signal and define the main characteristics of the circuit. I_O is copied to required branches using CMOS current mirrors.

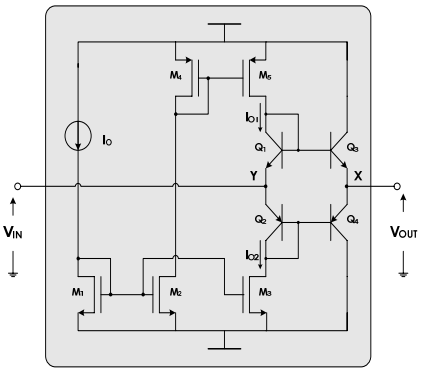

Figure 3 : Schematic representation of the new impedance matching circuit

The circuit contains one branch with 4 end-to-end junctions. A minimum polarity of 2.8V is thus required. Operating at ±1.5V has the evident advantage of low power consumption. Working at higher voltages reduces distortion and improves linearity. Preliminary analyses showed that the best performance was obtained at ±2.5V.

The control of R_X using I_O allows a matching circuit whose output impedance can be set to any desired value by simply varying the biasing current. In the classic conveyor, $R_X = V_T/2I_O$, where V_T is the thermal voltage [19],[22]. The control of R_{OUT} is thus continuous and easy to fine-tune.

SIMULATED PERFORMANCE

The active matching circuit was simulated using the transistor parameters of a 0.35µm SiGe-BiCMOS technology from STMicroelectronics. The transition frequency of the NPN transistors is 45GHz and that of PNP transistors is around 5GHz.

A. DC Performance

For the minimum polarisation required for the circuit, $V_{DC} = \pm 1.5V$, the total dissipation remains lower than 8mW and is inversely proportional to R_{OUT}. To obtain $R_{OUT} = 250\Omega$, only 0.9mW is dissipated. A truer indicator of dc performance is the current consumed by the circuit, I_{DC}. I_{DC} is similar for the two operating voltages: for $R_{OUT} = 200\Omega$, the current consumption is 0.57mA and 0.62mA at ±1.5V and ±2.5V respectively. For the entire range of R_{OUT}, I_{DC} remains lower than 4mA.

B. AC Performance

Fig. 4 shows the gain profiles at $V_{DC} = \pm 2.5V$. Ideally, the insertion of the impedance adaptation circuit does not affect the signal: the insertion loss is zero. However, any transistor-based circuit leads to a loss of signal (gain if it happens to be an amplifying circuit). Signal loss is much lower at ±2.5V operation than it is at ±1.5V: for $R_{OUT} = 50\Omega$, a loss of 0.36dB is observed at ±1.5V; at ±2.5V, it is only 0.01dB. The loss does not exceed 0.02dB for the range of R_{OUT} (50Ω to 250Ω).

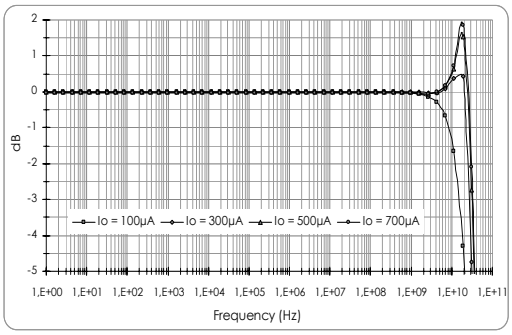

Figure 4 : Gain profiles (β versus frequency) at $V_{DC} = \pm 2.5V$

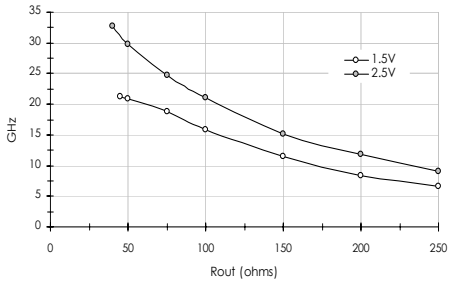

Figure 5 : -3dB cut-off frequencies; at $V_{DC} = \pm 1.5V$ and $\pm 2.5V$

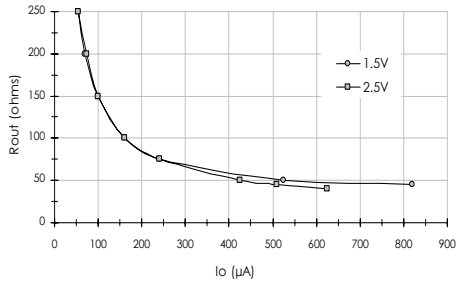

Figure 6 : Control of the output resistance R_{OUT} using the bias current I_O, at V_{DC} = ±1.5V and ±2.5V

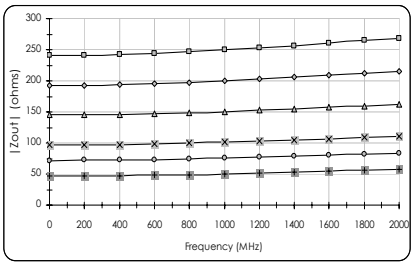

Figure 7 : $|Z_{OUT}|$ profiles versus frequency; at V_{DC} = ±2.5V

Classic passive-element matching circuits are intrinsically narrow-band (tuned to a particular frequency). Fig. 5 presents the -3dB bandwidths at the two operating voltages. For R_{OUT} = 50Ω, the -3dB bandwidths at ±1.5V and ±2.5V are, respectively, 20.9GHz (f_{TN}/2.2) and 29.8GHz (f_{TN}/1.5). The lower cut-off frequency is always zero.

C. Impedances

Z_{IN} is composed of resistance R_{IN} in parallel with capacitance C_{IN} (see fig. 2). R_{IN} is required to be as high as possible (ideally infinite) so that the signal loss due to the voltage divider (formed by the unmatched output impedance and R_{IN} of the matching circuit) is very low. At ±2.5V, R_{IN} is greater than 100kΩ.

Output impedance Z_{OUT} consists of two components: the desired resistive part (controlled using I_O, as shown in fig. 6) and an inductance L_{OUT}. This latter, however, does not exceed a few nH. For R_{OUT} = 50Ω, L_{OUT} is 1.8nH.

Fig. 6 presents the control of R_{OUT} using I_O. Below 40Ω for ±2.5V operation and 50Ω for ±1.5V operation, the potential of this impedance conversion circuit is reduced since its consumption goes up as R_{OUT} decreases.

The frequency variations never exceed 10% in the 0 – 2GHz range, and are inconsequential because any value of R_{OUT} can be obtained at any desired frequency, by fine-tuning I_O (fig. 7).

D. Linearity and compression point

A 50Ω load was connected to the matching circuit and the biasing conditions were fixed to give R_{OUT} = 50Ω, and the input power was varied in fixed steps to determine the linearity of the new circuit. It was observed that absolute linearity is maintained for all input signal powers up to 0dBm. In wireless communications transceivers, signal strengths almost never cross the upper limit of -20dBm. The impedance conversion circuit is linear up to powers (+11dBm) vastly beyond any signal that is likely to pass through it. For example, the RF components in [4], [23]-[25] have linearities much lower than this.

E. Scattering parameter performance

S-parameter analyses were carried out on the new matching circuit by terminating the two ports with a resistance R_{PORT} equal to R_{OUT}.

The input of the matching circuit is a voltage divider (between R_{PORT} and R_{IN}). Ideally, since $R_{IN} >> R_{PORT}$, there should be no loss of signal, and the signal strength across R_{IN} should be the same as that at the source. The input reflection coefficient S_{11} should therefore be one (0dB). It was observed that between 0 and 5GHz, S_{11} ranged from -0.15 to -1.72dB at ±2.5V, for all values of R_{PORT}.

It has already been seen (in the section on the AC performance) that a signal incident on the input port is very mildly attenuated: S_{21} has a value around -0.01dB.

A very small percentage of the incident signal traverses the circuit in the direction opposite to that intended: S_{12} remains lower than -15dB from 0 to 5GHz. The values of S_{12} are all the more remarkable for the fact that the isolation against the reverse signal is provided by only two transistors (either Q_1-Q_3 or Q_2-Q_4).

Fig. 8 presents the cardinal parameter of impedance matching circuits: the signal reflection at the output port. If R_{OUT} is perfectly matched to R_{PORT}, S_{22} assumes values that are very low. For impedance match to be considered 'successful', S_{22} must not exceed -10dB. The port impedances were varied for each value of I_O (and thus, for each desired R_{OUT} of the circuit). For each R_{OUT}, the matching is excellent up to 2GHz, with S_{22} lower than -12.5dB. The performance conforms to the accepted limits (-10dB) up to a frequency of 5GHz.

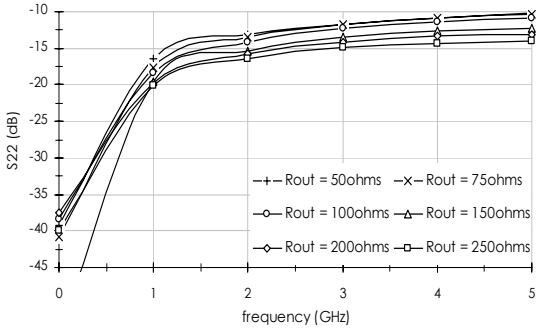

Figure 8 : S_{22} profiles for different R_{OUT}; at V_{DC} = ±1.5V

F. Temperature stability

All the above analyses were carried out while varying the circuit's temperature at regular intervals between -100°C and +100°C. For each analysis, the operating conditions are the same as those presented above. For brevity, only the results obtained for R_{OUT} = 50Ω are presented; similar performances were evinced for other values of R_{OUT}.

The insertion loss of the matching circuit varied from 0.008dB to 0.017dB at ±2.5V. The values at ambient temperature were, respectively, 0.363dB and 0.0126dB. At sub-zero temperatures, there was an improvement of the ac profile. At temperatures greater than +27°C, the ac gain degrades by only 0.03dB at both supplies.

The -3dB bandwidth showed an improvement for temperatures below +27°C. However, the most remarkable feature of these bandwidth-temperature profiles is the very low drop in bandwidth for temperatures higher than +27°C (15% drop for ±1.5V and 17% for ±2.5V).

For the two operating voltages, over the 200°C temperature range, S_{22} remained below -13dB.

G. *The matching circuit as a stand-alone device*

Measurements could not be carried out on the matching circuit as a stand-alone element because of the impedance limitations of the measurement apparatus. These apparatus require 50Ω terminations to reduce the reflection losses arising from the mismatch between the device's ports and the apparatus' ports. Since the input impedance of the matching circuit is ideally infinite, and practically much greater than the measurement apparatus' port impedance, any attempt at direct measurements on the matching circuit would have been futile because the signal fed by the apparatus would have been dissipated as reflection. Moreover, one of the two major applications of the new matching circuit (mentioned in the Introduction above) is to render the output of any RF circuit compatible with the measurement apparatus' ports, without degrading the performance of the circuit being studied. As such, we will not demonstrate the efficient matching between the LNA and the measurement apparatus.

The matching circuit is not destined to be a stand-alone element, but applicable to a wide range of RF components. In the next section, we present but one example of this application, for the sake of brevity. We have also applied this matching circuit to the outputs of several other wideband RF circuits (notably transistor-based baluns) and confirmed from the performances of these what we will observe for the LNA: the matching circuit provides wideband adaptation without deteriorating the performance or the physical characteristics of the circuit itself.

NEW MATCHING TECHNIQUE APPLIED TO LNA

The LNA that we have used as the target block is a three-transistor circuit. Its input is matched to 50Ω. Its gain is controllable from 0dB to 20dB, either continuously or in steps, using a control DC current. For this range of gains, the output impedance of the LNA varies from 50Ω to 500Ω. The intention behind the insertion of the matching circuit is to fix (using the biasing current of the matching circuit) the output impedance of the ensemble to 50Ω, and to make it independent of the gain control current.

A. *Effect of matching circuit on LNA performance*

The impedance matching circuit has an input resistance vastly superior (100 to 1000 times) to the LNA's output resistance. The loss of signal strength at the voltage divider formed by the input impedance of the matching circuit and the output impedance of the unmatched LNA should thus be negligible. The output impedance of the matching network is controlled by a current independent of the LNA's biasing currents, and the gain control of the LNA is not modified by the insertion of the matching network.

At 10dB gain, the unmatched LNA evinced -3dB bandwidths of DC to 2.8GHz. The addition of the matching circuit modified this to 2.4GHz. This can be attributed to the fact that the matched LNA contains PNP transistors which have very low transition frequencies. The transient signal's quality is preserved after the addition of the impedance matching circuit : the amplitude of the transient signal and its THD remain unchanged. The noise figure of the LNA is dictated by the first transistor in the signal chain. Since the impedance matching circuit is at the output of the LNA, its insertion does not modify the overall noise figure. Simulations verified that the total input-referred noise suffered no deterioration. The input match of the LNA to 50Ω was not disturbed. The presence of additional transistors in the main signal path led to an increased immunity to reverse signal propagation. This isolation, S_{12}, was improved by a constant factor of 15dB over the frequency range of DC to 5 GHz.

B. *Output Impedance Match*

The output impedance of the unmatched LNA was found to be 162Ω (for a gain of 10dB). The insertion of the matching network and the tuning of its biasing current led to the output impedance being perfectly matched to 50Ω. Fig. 9 presents the output reflection coefficient S_{22}, for a 50Ω system. The output of the LNA is ill-adapted to this standard impedance, as shown by the values of S_{22} for the unmatched LNA (S_{22} > -2dB). The insertion of the matching circuit changes the output of the LNA to 50Ω standard. S_{22} for the matched LNA is better than -12dB for the entire frequency range of DC to 5 GHz. For the entire range over which the gain is controllable, the output impedance shows a maximum variation of ±5% around 50Ω. The output impedance can also be set to values other than the standard 50Ω, if so desired, without engendering any loss in the performance of the LNA.

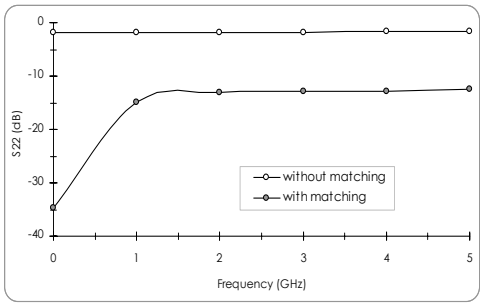

Figure 9 : Modification in S_{22} of LNA consequent to insertion of impedance matching circuit

C. *Measurement Results*

To further validate its application, the new impedance matching circuit was fabricated as part of the LNA in a 0.35µm SiGe-BiCMOS process. To render the LNA's output impedance constant, and independent of the gain control current, the new matching circuit was added at its output port. Fig. 10 shows a photograph of the new LNA, with its constituent elements. The total size of the LNA is 0.022mm², of which the matching circuit consumes 0.005mm². The result was a LNA that is perfectly matched to 50Ω, no matter what the value of its gain. Parameter S_{22} was lower than -11dB for all frequencies ranging from 0 to 5GHz. This adaptation is in perfect keeping with simulations (S_{22} < -10dB).

D. *Detailed performance of the LNA*

Since it would be beyond the scope of the paper to present detailed measurement results of the LNA's AC, noise and temperature performances, we will not include them. Moreover, the stand-alone LNA forms the subject of another publication proposal. However, the following remarks merit mention.

The AC performance of the LNA, as evinced by its gain and bandwidths, did not in the least suffer from the presence of the matching circuit, whose simulated insertion loss is next to zero (section V) and whose bandwidths extend from 0 to more than 10GHz.

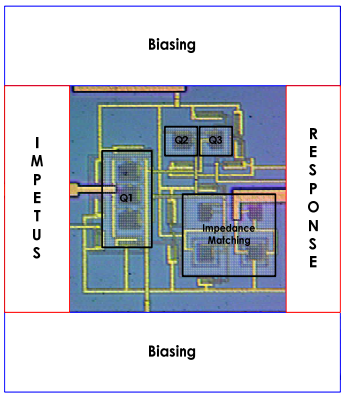

Figure 10 : Photograph of the LNA, showing the new output impedance matching circuit

The matching circuit is inserted at the output of the LNA (or any other RF block), in a cascade manner. Following Friis' law, the effect of the second element (the matching circuit) on the overall noise is decided by the noise of this matching circuit (which is low, as mentioned in section V) and the gain of the RF component itself (which ranges from 0 to 20dB, section VI). Comparisons between the matched and the unmatched LNA confirmed that the matching circuit has a negligible effect on the overall noise.

As concerns the temperature stability of the transistors and their models, detailed measurements were conducted on the final LNA to determine its temperature stability. The gain profiles and bandwidths were close over a 100°C temperature range from -25°C to +75°C: the gain profiles had less than 1dB variation for gains from 0 to 20dB; and the bandwidths were also stable. It is noteworthy that the performances improved at temperatures below the ambient 27°C. This is an indirect proof of the temperature stability of the impedance matching circuit.

COMPARISONS & CONCLUDING REMARKS

Existent output impedance matching circuits are currently implemented using LC networks, transformers, or quarter-wavelength lines, all of which present reflection zeros at particular frequencies and only allow matching in a narrow band around this frequency [6],[12],[16]. Table I presents one representative example of each type of impedance matching. The new impedance matching circuit is the first transistor-based topology ever observed, thus introducing a new class of solutions. It is by far the smallest among all the circuits. The LC network occupies at least half of the 0.24mm² chip area of the LNA in [6], while providing a moderate matching over a narrow band. Similarly, [12] has a transformer-based matching circuit which consumes a large fraction of the PA's 2.6mm² and achieves matching over a 500MHz range. [16] presents a λ/4-line impedance adapter which achieves matching between 0.4 and 1.6GHz, while using three transmission line sections. The area occupied by this circuit too, is quite high. On comparison with these, the new transistor-based matching circuit provides excellent matching over frequencies from 0 to at least 5GHz, while occupying only 0.005mm² on the chip. It is, therefore, the smallest output matching circuit ever, and one of the rare examples of wideband matching. The control of impedance (over the range 50Ω to 250Ω) is achieved using the biasing current; contrary to passive impedance matching networks, this control is flexible and does not necessitate the re-designing of the components. A wideband matching of a radio-frequency component's output can be achieved by the simple addition of the novel impedance matching circuit.

Table I : Comparative analyses of output matching circuits

Reference **Year**	**[6]** **2003**	**[14]** **2002**	**[12]** **2002**	**[16]** **2004**	**This work**
Type	LC-network	R-feedback	Transformer	λ/4 line	**Active**
Part of	LNA	LNA	PA	Stand-alone	**LNA**
Passives	2	4	1	-	**0**
Size	> 0.12mm²		> 1mm²		**0.005mm²**
Frequency range	5.65 – 5.85GHz	0 – 10GHz	2.15 – 2.65GHz	0.4 – 1.6GHz	**0 – 5GHz**
Output matching	< -8dB	< -10dB	- n.a. -	< -10dB	**< -11dB**

REFERENCES

[1] A. Bevilacqua, A. M. Niknejad; An Ultrawideband CMOS Low-Noise Amplifier for 3.1–10.6-GHz Wireless Receivers; IEEE Journal of Solid-State Circuits, Vol. 39, No. 12, December 2004; pp. 2259 – 2268.

[2] P. Andreani, H. Sjöland; Noise Optimization of an Inductively Degenerated CMOS Low Noise Amplifier; IEEE Transactions on Circuits and Systems – II : Analog and Digital Signal Processing, Vol. 48, No. 9, September 2001; pp. 835 – 841.

[3] F. Bruccoleri, E. A. M. Klumperink, B. Nauta; Wide-Band CMOS Low-Noise Amplifier Exploiting Thermal Noise Canceling; IEEE Journal of Solid-State Circuits, Vol. 39, No. 2, February 2004; pp. 275 – 282.

[4] Adiseno, M. Ismail, H. Olsson; A Wide-Band RF Front-End for Multiband Multistandard High-Linearity Low-IF Wireless Receivers; IEEE Journal of Solid-State Circuits, Vol. 37, No. 9, September 2002; pp. 1162 – 1168.

[5] F. Bruccoleri, E. A. M. Klumperink, B. Nauta,; Generating All Two-MOS-Transistor Amplifiers Leads to New Wide-Band LNAs; IEEE Journal of Solid-State Circuits, Vol. 36, No. 7, July 2001; pp. 1032 – 1040.

[6] D. J. Cassan, J. R. Long; A 1-V Transformer-Feedback Low-Noise Amplifier for 5-GHz Wireless LAN in 0.18-µm CMOS; IEEE Journal of Solid-State Circuits, Vol. 38, No. 3, March 2003; pp. 427 – 435.

[7] G. Girlando, G. Palmisano; Noise Figure and Impedance Matching in RF Cascode Amplifiers; IEEE Transactions on Circuits and Systems – II : Analog and Digital Signal Processing, Vol. 46, No. 11, November 1999; pp. 1388 – 1396.

[8] E. Abou-Allam, J. J. Nisbet, M. C. Maliepaard; Low-Voltage 1.9-GHz Front-End Receiver in 0.5-µm CMOS Technology; IEEE Journal of Solid-State Circuits, Vol. 36, No. 10, October 2001; pp. 1434 – 1443.

[9] H. Darabi, S. Khorram, H.-M. Chien, M.-A. Pan, S. Wu, S. Moloudi, J. C. Leete, J. J. Rael, M. Syed, R. Lee, B. Ibrahim, M. Rofougaran, A. Rofougaran; A 2.4-GHz CMOS Transceiver for Bluetooth; IEEE Journal of Solid-State Circuits, Vol. 36, No. 12, December 2001; pp. 2016 – 2024.

[10] H. Darabi, J. Chiu, S. Khorram, H. J. Kim, Z. Zhou, H.-M. Chien, B. Ibrahim, E. Geronaga, L. H. Tran, A. Rofougaran; A Dual-Mode 802.11b/Bluetooth Radio in 0.35-µm CMOS; IEEE Journal of Solid-State Circuits, Vol. 40, No. 3, March 2005; pp. 698 – 706.

[11] F. Ellinger; 26–42 GHz SOI CMOS Low Noise Amplifier; IEEE Journal of Solid-State Circuits, Vol. 39, No. 3, March 2004; pp. 522 – 528.

[12] I. Aoki, S. D. Kee, D. B. Rutledge, A. Hajimiri; Fully Integrated CMOS Power Amplifier Design Using the Distributed Active-Transformer Architecture; IEEE Journal of Solid-State Circuits, Vol. 37, No. 3, March 2002; pp. 371 – 383.

[13] R. Fujimoto, K. Kojima, S. Otaka; A 7-GHz 1.8-dB NF CMOS Low-Noise Amplifier; IEEE Journal of Solid-State Circuits, Vol. 37, No. 7, July 2002; pp. 852 – 856.

[14] M.-C. Chiang, S.-S. Lu, C.-C. Meng, S.-A. Yu, S.-C. Yang, Y.-J. Chan; Analysis, Design, and Optimization of InGaP–GaAs HBT Matched-Impedance Wide-Band Amplifiers With Multiple Feedback Loops; IEEE Journal of Solid-State Circuits, Vol. 37, No. 6, June 2002; pp. 694 – 701.

[15] J. M. Drozd, W. T. Joines; Using Parallel Resonators to Create Improved Maximally Flat Quarter-Wavelength Transformer Impedance-Matching Networks; IEEE Transactions on Microwave Theory and Techniques, Vol. 47, No. 2, February 1999; pp. 132 – 141.

[16] K. S. Ang, C. H. Lee, Y. C. Leong; A Broad Quarter-Wavelength Impedance Transformer with Three Reflection Zeros Within Passband; IEEE Transactions on Microwave Theory and Techniques, Vol. 52, No. 12, December 2004; pp. 2640 – 2643.

[17] S. E. Gunnarsson, C. Kärnfelt, H. Zirath, R. Kozhuharov, D. Kuylenstierna, A. Alping, C. Fager; Highly Integrated 60 GHz Transmitter and Receiver MMICs in a GaAs pHEMT Technology; IEEE Journal of Solid-State Circuits, Vol. 40, No. 11, November 2005; pp. 2174 – 2186.

[18] H. Darabi, et al.; "A Dual-Mode 802.11b/Bluetooth Radio in 0.35µm CMOS"; IEEE Journal of Solid- State Circuits, Vol. 40, No. 3, March 2005; pp. 698 – 706.

[19] A. Fabre, O. Saaid, F. Wiest, C. Boucheron; High-frequency applications based on a new current controlled conveyor; IEEE Transactions on Circuits and Systems – I : Fundamental Theory and Applications, Vol. 43, No. 2, February 1996; pp. 82 – 91.

[20] F. Seguin, B. Godara, F. Alicalapa, A. Fabre; 2.2 GHz All-n-p-n Second-Generation Controlled Conveyor in Pseudoclass AB Using 0.8-µm BiCMOS Technology; IEEE Transactions on Circuits and Systems – II : Express Briefs, Vol. 51, No. 7, July 2004; pp. 369 – 373.

[21] F. Seguin, A. Fabre; New Second Generation Current Conveyor with Reduced Parasitic Resistance and Bandpass Filter Application; IEEE Transactions on Circuits and Systems – I : Fundamental Theory and Applications, Vol. 48, No. 6, June 2001; pp. 781 – 785.

[22] A. Fabre, M. Alami, A. Boudhada ; Second Generation Current Conveyors with Enhanced Input Resistance ; International Journal of Electronics, Vol. 86, 1999; pp. 405 – 412.

[23] F. Gatta, et al.; "A 2-dB Noise Figure 900-MHz Differential CMOS LNA"; IEEE Journal of Solid-State Circuits, Vol. 36, No. 10, October 2001; pp. 1444 – 1452.

[24] A. Liscidini, et al; "A 0.13µm CMOS Front-End, for DCS1800/UMTS/802.11b-g With Multiband Positive Feedback Low-Noise Amplifier"; IEEE JSSC, Vol. 41, No. 4, Apr. 2006; pp. 981 – 989

[25] M. P. van der Heijden, et al; "On the Design of Unilateral Dual-Loop Feedback Low-Noise Amplifiers with Simultaneous Noise, Impedance, and IIP3 Match"; IEEE JSSC, Vol. 39, No. 10, Oct. 2004; pp. 1727 – 1736